Title

Probing Electron Transfer in the Manganese-Oxide-Forming MnxEFG Protein Complex using Fourier Transformed AC Voltammetry: Understanding the Oxidative Priming Effect

Journal

ChemElectroChem, 5(6)

ISSN

2196-0216

Authors

Tao, Lizhi
Simonov, Alexandr N
Romano, Christine A
et al.

Publication Date

2018-03-15

DOI

10.1002/celc.201700563

Peer reviewed

ChemPubSoc Europe

DOI: 10.1002/celc.201700563

CHEMELECTROCHEM Articles

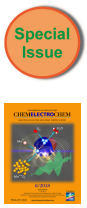

Probing Electron Transfer in the Manganese-Oxide-Forming MnxEFG Protein Complex using Fourier Transformed AC Voltammetry: Understanding the Oxidative Priming Effect

Lizhi Tao[+],[a] Alexandr N. Simonov[+],*[b, c] Christine A. Romano,[d] Cristina N. Butterfield,[d] Bradley M. Tebo,[d] Alan M. Bond,[b, c] Leone Spiccia,[b, c] Lisandra L. Martin,*[b] and William H. Casey*[a, e]

Leone Spiccia passed away prior to submission of this paper. He was an esteemed colleague of ours and is sadly missed.

MnxG, a multicopper oxidase, is an enzyme from the marine *Bacillus* species, which produces manganese oxide minerals through the aerobic oxidation of dissolved Mn^{2+} – a key process in global manganese geochemical cycling. When isolated in an active form as a part of the MnxEFG protein complex, the enzymatic activity of MnxG is substantially enhanced by mild oxidative priming. Herein, the mechanism for this effect is probed by using direct current (dc) and Fourier transformed alternating current (ac) voltammetric analysis of the MnxEFG complex and the catalytically inactive MnxEF subunit immobilised on a carbon electrode. Analysis of these ac voltammetric data reveals a significant enhancement in the rate of electron transfer in the Type 2 Cu sites upon oxidative priming of the enzyme, which is attributed to the improved catalytic activity of MnxG in the MnxEFG protein complex.

1. Introduction

The significance of manganese oxide minerals (MnO_x) in technology and the environment can be hardly overestimated.[1–3] Thus, understanding the mechanism of formation and global geochemical cycling of MnO_x is a critical scientific problem, where significant progress has been achieved over the last few decades.[4–6] In particular, an essential role of bacteria and fungi in mineralisation of MnO_x has been established, and microbial oxidation of dissolved $Mn^{2+}_{(aq)}$ by dissolved oxygen has been suggested as one pathway for the formation of these minerals in the ocean.[5,6] A gene that enables the marine *Bacillus* species (PL-12, SG-1 and MB-7) to facilitate oxidation of Mn^{2+} to MnO_x is *mnxG*, which encodes a putative multicopper oxidase. The product of this gene, MnxG, has been successfully overexpressed and isolated in an enzymatically active form as a part of the MnxEFG protein complex,[7] which has a molecular weight of ca 211 kDa and contains two accessory proteins, MnxE and MnxF, that do not exhibit enzymatic activity towards MnOx biomineralisation.[8,9]

Mechanistic studies using electron paramagnetic resonance spectroscopy confirmed that the mechanism of the MnxG-catalysed aerobic oxidation of Mn^{2+} is akin to that for oxidation of organic substrates catalysed by smaller multicopper oxidases.[10] In brief, three types of copper cofactors are needed to catalyse four sequential single-electron oxidations of substrates coupled to the four-electron reduction of O_2 to H_2O.[11,12] These cofactors are Type 1 "blue" copper (T1Cu) which oxidises the substrate and transfers electrons to the Type 2 "normal" copper (T2Cu) and "coupled binuclear" Type 3 copper (T3Cu) sites that act cooperatively to bind and reduce dioxygen to water.

In order to obtain further insights into the enzymatic mechanism of MnxG, electrochemical and kinetic studies have been undertaken, as reported in our recent publication.[8] Direct current (dc) and Fourier transformed (FT) alternating current (ac) voltammetric[13,14] analysis of MnxEF immobilised on the self-assembled monolayer of 6-mercaptohexanoic acid (MHA) on a Au electrode have provided values of the apparent (effective) reversible potentials (E_{app}) for the T2Cu sites in these

[a] *Dr. L. Tao,[+] Prof. Dr. W. H. Casey*
Department of Chemistry
University of California
One Shields Avenue, Davis, California 95616, United States
E-mail: whcasey@ucdavis.edu
[b] *Dr. A. N. Simonov,[+] Prof. Dr. A. M. Bond, Prof. Dr. L. Spiccia, Prof. Dr. L. L. Martin*
A School of Chemistry
Monash University, Victoria 3800, Australia
E-mail: alexandr.simonov@monash.edu
lisa.martin@monash.edu
[c] *Dr. A. N. Simonov,[+] Prof. Dr. A. M. Bond, Prof. Dr. L. Spiccia*
ARC Centre of Excellence for Electromaterials Science
Monash University, Victoria 3800, Australia
[d] *Dr. C. A. Romano, Dr. C. N. Butterfield, Prof. Dr. B. M. Tebo*
Division of Environmental and Biomolecular Systems
Institute of Environmental Health
Oregon Health & Science University
Portland, Oregon 97239, United States
[e] *Prof. Dr. W. H. Casey*
Department of Earth and Planetary Sciences
University of California
One Shields Avenue, Davis, California 95616, United States
[+] *These authors contributed equally to this work*
An invited contribution to the Alan Bond Festschrift

subunits as 0.33–0.35 V *vs.* normal hydrogen electrode (NHE; hereinafter all potentials are provided *vs.* this reference). For MnxEFG, direct electron transfer between Cu sites and the electrodes has been also established, though the unambiguous assignment of the faradaic processes to either T1Cu or T2/T3Cu was not possible. Most interestingly, the enzymatic activity of MnxEFG was found to substantially improve upon mild voltammetric oxidation of the protein complex adsorbed on a carboxy-terminal monolayer. However, establishing the origins of *oxidative priming* was not possible as MHA/Au produces strong background voltammetric signals when oxidised, which overlap with the response from the Cu sites and complicate the interpretation of the data. In the present communication, we describe an extended voltammetric analysis using a stable carbon-based support to immobilise MnxEFG that enables new insights to be gained into the mechanism of the oxidative priming.

2. Results and Discussion

As background information to this study, it is useful to outline the basic principles of FT ac voltammetry, and also to consider the changes in the dc and ac voltammetric responses for the MHA/Au electrodes induced by electrooxidation. In a typical large amplitude ac voltammetric experiment, a potential waveform is constructed as a combination of a linear sweep (as in dc voltammetry) and a periodic perturbation, for example a sinusoid with an amplitude $\Delta E > 0.05$ V and a frequency $9 \leq f <$ 1000 Hz. When applied to a redox system where a faradaic process occurs, such waveform generates a non-linearity in the current response. In other words, the resulting current-time response is comprised of an aperiodic (dc) component, a periodic fundamental harmonic having frequency *f*, and also periodic components with frequencies 2*f*, 3*f*, etc. (higher order harmonics). The FT – band selection and filtering – inverse FT sequence of operations can then be applied to extract and analyse each component individually. Among many other applications, FT ac voltammetry is particularly useful for studies on the surface-confined phenomena where faradaic current is comparable or lower in magnitude than the background capacitive response. Indeed, higher order harmonics (e.g. 4th considered in this study) exhibit close to zero background and are dominated by the faradaic current, whose magnitude is highly sensitive to the rate of electron transfer. Further details are available from recent publications.[13,14]

Figure 1 compares the evolution of the dc and ac voltammetric responses for the bare and MnxEFG-modified MHA/Au electrodes upon cycling the potential from 0.05–0.20 V to 0.75–0.90 V. Substantial faradaic currents develop within the potential range 0.30–0.60 V when MHA/Au is electrooxidised. Adsorption of MnxEFG on this oxidised electrode partially suppresses these signals both in dc and ac components and produces new well-defined dc reduction (R1 at *ca* 0.25 V) and oxidation (O1 at *ca* 0.50 V) processes (Figure 1a, blue trace), which are similar to those obtained using intact MHA/Au support.[8] As explained

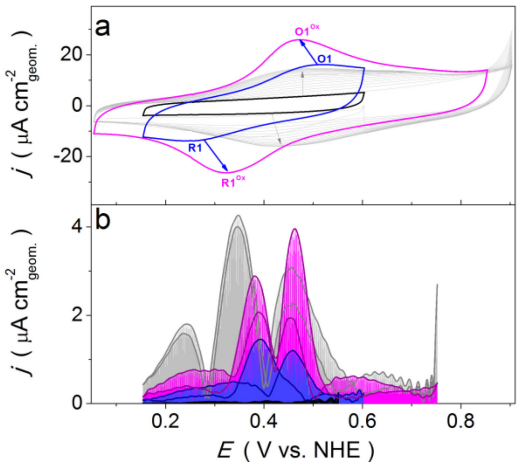

Figure 1. Voltammetry for the MnxEFG protein complex immobilised on a Au electrode modified with a monolayer of 6-mercaptohexanoic acid in contact with air-saturated aqueous 500 mM NaCl + 20 mM HEPES (pH = 7.8). a) Dc voltammograms ($v = 0.10$ V s^{-1}) and b) 4th harmonics of ac voltammograms ($f = 9.02$ Hz; $\Delta E = 0.08$ V; $v = 0.034$ or 0.045 V s^{-1}) for a bare (*black* and *grey*) and MnxEFG-modified electrode (*blue* and *magenta*). Experiment giving rise to the *black* curve was undertaken first. Data represented by *grey* colour were then obtained. Next, MnxEFG was adsorbed on the oxidised electrode and the *blue* voltammetric response was recorded. Finally, the MnxEFG-modified electrode was again oxidised by cycling the potential from 0.17 to 0.85 V (*magenta*). Arrows show changes induced by electrooxidation of the electrode. In panel b, *dark grey*, *purple* and *navy* curves display the envelope form for the corresponding ac current.

previously,[8] the contribution of Cu cofactors of MnxEFG to R1 and O1 is most probably insignificant. In the ac components (exemplified in the 4th harmonic in Figure 1b, magenta trace), it is not possible to identify the weak response expected from Cu sites as in experiments undertaken with the non-oxidised MHA/Au electrode.[8]

Continuous cycling of the potential of the MnxEFG/MHA/Au electrode from 0.17 to 0.85 V induces further notable changes in the voltammograms. In particular, the dc peak-to-peak separation is reduced and the magnitudes of the dc R1 and O1 currents are enhanced (Figure 1a), as are the ac faradaic currents (*cf.* magenta and blue data in Figure 1b). However, unambiguous assignment of contributions from further oxidation-induced transformations of the MHA/Au support and putative changes in the electron transfer in MnxEFG cannot be made on the basis of these data.

To overcome the limitations of the MHA-modified Au electrode, we immobilised the MnxEFG protein complex on the carbon black (Vulcan-XC72) support, which allows the positive potential range to be probed in more detail (Figures 2 and 3a). The MnxEFG-modified carbon-based electrode produced a set of dc signals (R1/O1 in Figure 2a) and also a small ac response in the 0.30–0.40 V range (R2/O2 in Figure 2b, blue trace). Importantly, these voltammetric responses qualitatively resemble the data obtained for the protein complex adsorbed on non-oxidised MHA/Au.[8] On this basis, small ac R2/O2 processes in Figure 2b can be ascribed to the redox transformations of T2Cu in MnxEF and undefined Cu sites in MnxG. However, the origin of the dc R1/O1 redox processes remains unclear. The fact that adsorption of MnxEFG on carbon black and MHA/Au

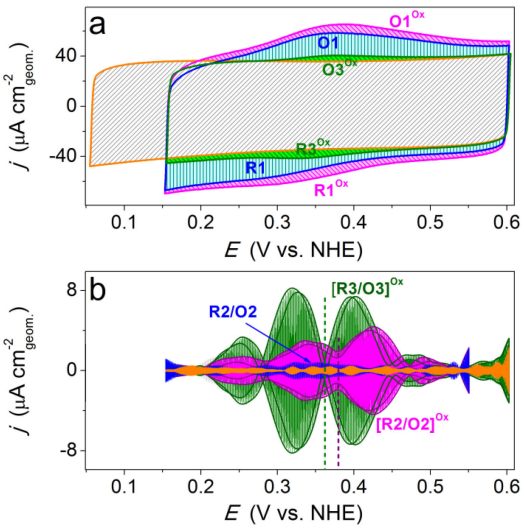

Figure 2. Voltammetry for the MnxEFG protein complex and the MnxEF subunit adsorbed on carbon black. a) Dc voltammograms ($v = 0.10\ V\,s^{-1}$) and b) 4th harmonics of ac voltammograms ($f = 9.02$ Hz; $\Delta E = 0.08$ V; $v = 0.034$ or $0.045\ V\,s^{-1}$) for bare (*grey*), and MnxEFG- (*blue*) or MnxEF-modified (*orange*) electrodes. The effect of cycling the potential from 0.15 to 0.90 V is shown for MnxEFG (*magenta*) and MnxEF-modified (*green*) electrodes. Dc voltammograms highlighted with hatched area define charges associated with background processes (*grey*), MnxEFG (*cyan* + *blue*), oxidatively activated MnxEF (*green*) and MnxEFG (*magenta*). Solid *dark green* and *purple* curves in (b) represent envelopes of the *green* and *magenta* voltammetric data, respectively. Dashed lines indicate approximate values of E_{app} for $[R2/O2]^{Ox}$ (*purple*) and $[R3/O3]^{Ox}$ (*green*).

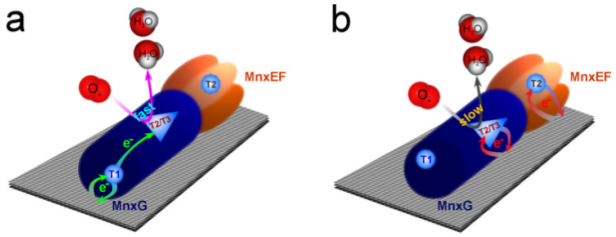

Scheme 1. A schematic representation of electron transfer from the electrode (*grey*) to the MnxEFG protein complex. a) A hypothetical situation in the multicopper oxidase MnxG unit, where direct electron transfer between the electrode and the T1Cu site is possible, thus enabling intramolecular electron transfer from T1Cu to the T2/3Cu site and enzymatic reduction of molecular oxygen similar to laccase and other smaller multicopper oxidases. b) The postulated scenario observed experimentally. Electron transfer between T2Cu sites in MnxEF subunit and electrode is also possible, which is omitted in (a).

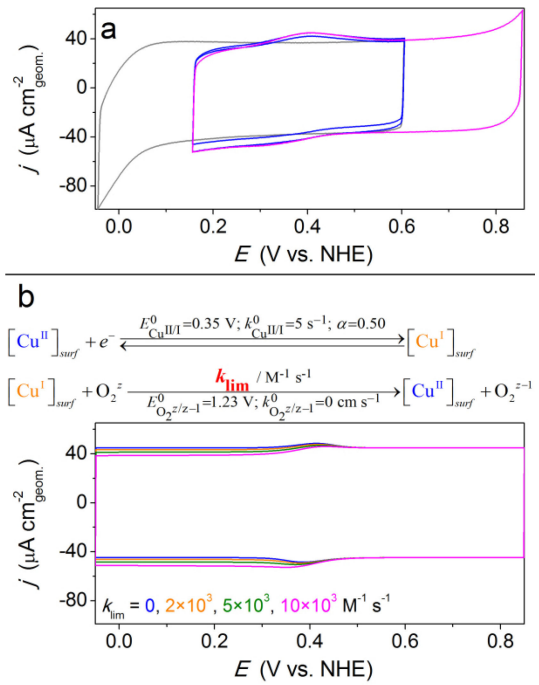

Figure 3. Comparison of the dc voltammetry ($v = 0.100\ V\,s^{-1}$) for the MnxEFG-modified electrode in contact with air- and N_2-saturated electrolyte solutions. a) Electrode formed from carbon black Vulcan-XC72 deposited on glassy carbon (*grey*) and the same electrode after modification with MnxEFG (*blue* and *magenta*) in contact with air-saturated (*grey* and *magenta*) or N_2–saturated (*blue*) 500 mM NaCl + 20 mM HEPES aqueous solution (pH = 7.8). Dashed *blue* curve represents the original data, whereas that given in the solid *blue* curve has been scaled to facilitate comparisons. b) Simplified representation of the mechanism for the oxygen reduction reaction and simulated data based thereon. Simulation parameters: E^0 – standard reversible potential; k^0 – heterogeneous electron transfer rate constant; α – charge transfer coefficient (Butler-Volmer model); k_{lim} – catalytic rate constant; surface concentration of Cu 40 pmol cm^{-2}; concentration and diffusion coefficient of dissolved 'oxygen' 0.2 mM and 2×10^{-5} cm^2 s^{-1}; electrode surface area 0.067 cm^2; double-layer capacitance 450 μF cm^{-2}; uncompensated resistance 0 Ω; temperature 298 K. Note that some simulated voltammograms are hard to distinguish at the resolution of this figure.

produces similar voltammetry is an important observation. It allows us to deduce that changes in the enzymatic activity detected by quartz crystal microbalance and a MHA/Au platform[8] correlate with changes in electrochemical response obtained with the carbon-based electrode as discussed later in the text.

An important feature to note in data provided in Figures 1a and 3a is the absence of fast electrocatalytic reduction of molecular oxygen when the MnxEFG protein complex is adsorbed either on carbon or MHA/Au. This result contrasts with studies on laccase and other small multicopper oxidases where well-defined cathodic current associated with the protein-catalysed O_2 reduction is reported.[15–18] In these cases, the electrocatalytic capacity was provided by the direct electron transfer between the electrode and the T1Cu sites of the enzymes. Electrons supplied to T1Cu from the electrode were further tunneled *via* the natural intramolecular electron transfer pathway to the T2/3Cu cofactors where fast O_2 reduction ($k_{eff} \approx 10^6\ M^{-1}\,s^{-1}$) occured (exemplified in Scheme 1a).[19–23] Obviously, fast dioxygen reduction does not occur with the MnxEFG complex since the voltammetric response is not strongly influenced by the presence of dissolved O_2 under conditions employed here (Figure 3a) or previously.[8] This result suggests that the T1Cu site in the MnxG unit is inaccessible for the direct electron transfer from the electrode. Thus, we attribute the R2/O2 ac voltammetric signals in Figure 2b and Figure 2b of Ref.[8] to the $T2/3Cu^{I/II}$ processes in the MnxG unit (as is common for multicopper oxidases, distinction between the voltammetric responses from T2Cu and T3Cu is difficult[24]) with a contribution from $T2Cu^{I/II}$ of MnxEF.

In principle, electroreduction of dissolved O_2 at the T2/3Cu sites of multicopper oxidases *via* direct electron transfer from the electrode is also possible, but typically at substantially slower rates than achieved by the enzymatic process.[19,21–23] However, slow electroreduction may not be detectable under conditions relevant to the present study. To evaluate the sensitivity of the voltammetric form of analysis, simulations were carried out (Figure 3b). This theoretical analysis suggests that differences in dc voltammograms obtained for the adsorbed MnxEFG complex in air-saturated and oxygen-free solutions would not be experimentally detectable when the rate constant for the reaction between dissolved O_2 and the reduced state of the catalyst (i.e. T2/3Cu^{I}) is below *ca.* $2\times10^3\ M^{-1}s^{-1}$. Therefore, our data cannot exclude the possibility that the T2/3Cu site of MnxG unit can catalyse reduction of oxygen, though if present, this process must occur at a relatively slow rate when the electrons are supplied to the catalytic site directly from the electrode rather than from the T1Cu site (Scheme 1).

The impact of electrooxidation of the MnxEFG complex and the MnxEF subunit adsorbed on carbon black is shown in Figure 2. Application of mildly positive potentials of 0.85–0.90 V for only a few seconds enhances the dc and especially the ac responses from the proteins, and the new processes generated are labelled with superscripts "Ox". It is difficult to distinguish contributions from the MnxEF and MnxG units using the dc voltammograms, but the FT ac voltammetric data provide important insights. The significant increase in the ac response (as exemplified for the 4th ac harmonic components in Figure 2b) reflects a dramatic enhancement in the rate of electron transfer[14] within the redox-active sites of the protein, in particular T2Cu in MnxEF with $E_{app}=0.36$ V ([R3/O3]^{Ox} in Figure 2b). Enhancement of the electron transfer kinetics in the copper sites of the MnxEFG complex is detectable when potentials more positive than 0.65–0.70 V are applied for up to 20 min (data not shown). However, achieving a significant effect over a short period of time requires potentials above 0.80–0.85 V. The slightly distorted and asymmetrical ac response from the MnxEFG complex ([R2/O2]^{Ox} in Figure 2b) is attributed to an unresolved combination of processes at the T2Cu$^{I/II}$ site in the MnxEF subunit and the T2/3Cu$^{I/II}$ site in the MnxG unit. By comparing the ac responses from the oxidised MnxEF subunit and the MnxEFG complex, E_{app} for the activated T2/3Cu$^{I/II}$ process in MnxG is estimated to fall within the 0.36–0.40 V range, consistent with the value for the MnxG unit adsorbed on a carboxy-terminal monolayer on gold.[8]

The above voltammetric analysis reveals that oxidative priming of the MnxEFG protein complex does not induce significant changes in E_{app} for T2/3Cu$^{I/II}$ but actuates faster electron transfer within these sites. Facilitation of the electron transfer can now be invoked to rationalise the *oxidative priming* effect, i.e. significant acceleration of the MnO_x mineralisation catalysed by electrooxidised MnxEFG as compared to the reaction in the presence of the as-isolated protein complex.[8] As expected, oxidation of the MnxEF subunit does not affect its activity as it is already known to be unable to catalyse MnO_x formation.[9]

3. Conclusions

Analysis of dc and FT ac voltammetric data for MnxEFG immobilised on the carboxy-terminal monolayer on gold and carbon-black supports suggests that the enhancement in the enzymatic activity of this manganese-oxidising protein complex induced by oxidative priming is associated with facilitated electron transfer within the T2 and T2/3Cu cofactors. In principle, applying positive potentials could generate a conformational change of the protein or modify the ligand environment of the T2/3Cu sites in the MnxG unit. Either change could lead to lower reorganisation energy for intramolecular electron transfer from T1Cu to T2/3Cu sites after oxidative priming.

Experimental Section

Materials

Analytical grade chemicals were purchased either from Sigma-Aldrich or Merck and used as received. High-purity water (Sartorius, 18 MΩ cm at 25 °C) and N_2 (99.999 %, $O_2<2$ ppm) were used.

Proteins

The MnxEFG protein complex (*mnx*E_3F_3G, *ca.* 211 kDa) and the MnxEF subunits (*mnx*EF, *ca.* 73 kDa) were obtained by expressing the *Bacillus* sp. PL-12 *mnx*DEFG operon in *E. coli* and a plasmid encoding just the *mnxE* and *mnxF* genes, respectively. Detailed procedures are available elsewhere.[9]

Voltammetric Studies

Voltammetric studies were undertaken using a BAS Epsilon electrochemical workstation and a custom-built FT ac voltammetry instrument[25] in a three-electrode Pyrex cell at 23 ± 2 °C. Prior to use, all glassware was soaked in H_2SO_4 (98 wt.%): H_2O_2 (30 vol.%) (1 : 1 vol.) for more than 12 h, washed with water and dried at 110 °C in air. Measurements were undertaken using 500 mM NaCl + 20 mM 4-(2-Hydroxyethyl)piperazine-1-ethanesulfonic acid (HEPES) electrolyte solutions (pH = 7.8) that were either N_2- or air-saturated.

The high-surface-area Pt auxiliary electrode was separated from the main compartment with a low-porosity glass frit. A AgCl-coated Ag wire placed inside a Luggin capillary and immersed directly in the working electrolyte solution was used as a reference electrode, as required for the high-quality ac voltammetric measurements.[13,14] The potential of this low-impedance Ag | AgCl | 500 mM NaCl + 20 mM HEPES configuration was stable at 0.057 ± 0.001 V *vs.* Ag | AgCl | KCl(sat.) or 0.254 ± 0.001 V *vs.* NHE, which agrees well with the Nernst equation.

A glassy carbon (GC; BAS, diameter 0.3 cm) and Au electrodes (BAS; diameter 0.2 cm) were used as substrates to prepare modified working electrodes. Prior to use, the GC and Au surfaces were polished with an aqueous slurry of Al_2O_3 powder (Buehler; 0.3 μm) on a wet polishing cloth (BAS), copiously washed with water, ultrasonicated in water for 20–30 s (FXP 10 M, U-LAB Instruments, Australia), wiped *ca* 50 times with a clean wet polishing cloth, ultrasonicated for an additional 20–30 s in a fresh portion of water, and washed with water again.

A glassy carbon electrode was used as a substrate for deposition of a thin layer of a Vulcan-XC72 carbon black

(Brunauer–Emmett–Teller specific area 222 $m^2 g^{-1}$). This was achieved by applying 5–10 µl of a 0.6 mg ml^{-1} suspension of the carbon material in isopropanol : H_2O (2:3 vol.) mixture and slowly drying under a N_2 flow. Prior to deposition, the suspension was ultrasonicated for *ca.* 30 min. A Au electrode was used to create a carboxy-terminal surface by adsorbing a monolayer of 6-mercaptohexanoic (MHA) acid from the 1 mM solution in isopropanol for at least 1 h. To ensure a clean surface of Au before modification with MHA, the electrode was first cleaned electrochemically by recording cyclic voltammograms within the potential range 0.2–1.5 V *vs.* NHE in 0.1 M H_2SO_4 at $v = 0.020$ V s^{-1} until a stable response that is typical of polycrystalline gold was achieved.

After voltammetric characterisation of Vulcan-XC72/GC or MHA/Au electrodes, either MnxEFG or MnxEF was adsorbed on the surface by applying 5 µL of the 0.14 mM protein solutions in 50 mM NaCl + 20 mM HEPES (pH = 7.8) and keeping the electrodes under a gentle N_2 flow for 15 min.

Acknowledgements

The work was supported by NSF grants EAR1231322 (WHC and LS) and CHE1541202 (BMT), the Australian Research Council through the ARC Centre of Excellence for Electromaterials Science (CE140100012 to LS), and an NSF Postdoctoral Research Fellowship in Biology Award ID: DBI-1202859 to CAR.

Conflict of Interest

The authors declare no conflict of interest.

Keywords: MnO_x mineralisation · electron transfer · multicopper oxidase · direct current protein voltammetry · Fourier transformed alternating current voltammetry

[1] E. D. Goldberg, *J. Geol.* **1954**, *62*, 249–265.
[2] J. E. Post, *Proc. Natl. Acad. Sci. USA.* **1999**, *96*, 3447–3454.
[3] M. M. Najafpour, M. Hołyńska, S. Salimi, *Coord. Chem. Rev.* **2015**, *285*, 65–75.
[4] W. G. Sunda, S. A. Huntsman, *Deep-Sea Res.* **1988**, *35*, 1297–1317.
[5] B. M. Tebo, J. R. Bargar, B. G. Clement, G. J. Dick, K. J. Murray, D. Parker, R. Verity, S. M. Webb, *Annu. Rev. Earth Planet. Sci.* **2004**, *32*, 287–328.
[6] T. G. Spiro, J. R. Bargar, G. Sposito, B. M. Tebo, *Acc. Chem. Res.* **2010**, *43*, 2–9.
[7] C. N. Butterfield, A. V. Soldatova, S.-W. Lee, T. G. Spiro, B. M. Tebo, *Proc. Natl. Acad. Sci. USA* **2013**, *110*, 11731–11735.
[8] L. Tao, A. N. Simonov, C. A. Romano, C. N. Butterfield, M. Fekete, B. M. Tebo, A. M. Bond, L. Spiccia, L. L. Martin, W. H. Casey, *Chem. – Eur. J.* **2017**, *23*, 1346–1352.
[9] C. N. Butterfield, L. Tao, K. N. Chacón, T. G. Spiro, N. J. Blackburn, W. H. Casey, R. D. Britt, B. M. Tebo, *Biochim. Biophys. Acta, ProteinsProteomics* **2015**, 1854, 1853–1859.
[10] L. Tao, T. A. Stich, C. N. Butterfield, C. A. Romano, T. G. Spiro, B. M. Tebo, W. H. Casey, R. D. Britt, *J. Am. Chem. Soc.* **2015**, *137*, 10563–10575.
[11] E. I. Solomon, U. M. Sundaram, T. E. Machonkin, *Chem. Rev.* **1996**, *96*, 2563–2606.
[12] E. I. Solomon, R. K. Szilagyi, S. DeBeer George, L. Basumallick, *Chem. Rev.* **2004**, *104*, 419–458.
[13] A. M. Bond, D. Elton, S.-X. Guo, G. F. Kennedy, E. Mashkina, A. N. Simonov, J. Zhang, *Electrochem. Comm.* **2015**, *57*, 78–83.
[14] A. M. Bond, E. A. Mashkina, A. N. Simonov in *Developments in Electrochemistry: Science Inspired by Martin Fleischmann* (Eds.: D. Pletcher, Z.-Q. Tian, D. Williams, D.) John Wiley & Sons, Ltd: New York, **2014**, p 21-47.
[15] L. Santos, V. Climent, C. F. Blanforda, F. A. Armstrong, *Phys. Chem. Chem. Phys.* **2010**, *12*, 13962–13974.
[16] S. Shleev, J. Tkac, A. Christenson, T. Ruzgas, A. Yaropolov, J. W. Whittaker, L. Gorton, *Biosens. Bioelectron.* **2005**, *20*, 2517–2554.
[17] Y. Kamitaka, S. Tsujimura, K. Kataoka, T. Sakurai, T. Ikeda, K. Kano, *J. Electroanal. Chem.* **2007**, *601*, 119–124.
[18] D. L. Johnson, J. L. Thompson, S. M. Brinkmann, K. A. Schuller, L. L. Martin, *Biochem.* **2003**, *42*, 10229–10237.
[19] S. K. Lee, S. D. George, W. E. Antholine, B. Hedman, K. O. Hodgson, E. I. Solomon, *J. Am. Chem. Soc.* **2002**, *124*, 6180–6193.
[20] D. L. Johnson, J. L. Thompson, S. M. Brinkmann, K. A. Schuller, L. L. Martin, *Biochemistry.* **2003**, *42*, 10229–10237.
[21] E. I. Solomon, A. J. Augustine, J. Yoon, *Dalton Trans.* **2008**, *30*, 3921–3932.
[22] D. E. Heppner, C. H. Kjaergaard, E. I. Solomon, *J. Am. Chem. Soc.* **2013**, *135*, 12212–12215.
[23] J. Li, M. Farrokhnia, L. Rulíšell, U. Ryde, *J. Phys. Chem. B.* **2015**, *119*, 8268.
[24] S. Shleev, A. Christenson, V. Serezhenkov, D. Burbaev, A. Yaropolov, L. Gorton, T. Ruzgas, *Biochem. J.* **2005**, *385*, 745–754.
[25] A. M. Bond, N. W. Duffy, S.-X. Guo, J. Zhang, D. Elton, *Anal. Chem.* **2005**, *77*, 186A–195A.

Manuscript received: June 6, 2017
Accepted Article published: July 12, 2017
Version of record online: August 10, 2017